Phloroglucinol-enhanced whey protein isolate hydrogels with antimicrobial activity for tissue engineering

Varvara Platania [a,b], Timothy E.L. Douglas [c,d,*], Mikhajlo K. Zubko [e], Danny Ward [f], Krzysztof Pietryga [g], Maria Chatzinikolaidou [a,b,**]

[a] Dept. of Materials Science and Technology, University of Crete, 70013 Heraklion, Greece
[b] Foundation for Research and Technology Hellas (FORTH)-Institute of Electronic Structure and Laser (IESL), 70013 Heraklion, Greece
[c] Engineering Department, Lancaster University, UK
[d] Materials Science Institute (MSI), Lancaster University, UK
[e] Centre for Bioscience, Manchester Metropolitan University (MMU), Manchester, UK
[f] Department of Biological and Life Sciences (BLS), Lancaster University, UK
[g] Department of Biomaterials and Composites, AGH University of Science and Technology, Krakow, Poland

Keywords:
Whey protein
Phloroglucinol
Hydrogels
Osteogenic differentiation
Cytocompatibility
Dental pulp stem cells
MG-63 cells
Antimicrobial activity

Aging populations in developed countries will increase the demand for implantable materials to support tissue regeneration. Whey Protein Isolate (WPI), derived from dairy industry by-products, can be processed into hydrogels with the following desirable properties for applications in tissue engineering: (i) ability to support adhesion and growth of cells; (ii) ease of sterilization by autoclaving and (iii) ease of incorporation of poorly water-soluble drugs with antimicrobial activity, such as phloroglucinol (PG), the fundamental phenolic subunit of marine polyphenols.

In this study, WPI hydrogels were enriched with PG at concentrations between 0 and 20% *w/v*. PG solubilization in WPI hydrogels is far higher than in water. Enrichment with PG did not adversely affect mechanical properties, and endowed antimicrobial activity against a range of bacteria which occur in healthcare-associated infections (HAI). WPI-PG hydrogels supported the growth of, and collagen production by human dental pulp stem cells and - to a lesser extent - of osteosarcoma-derived MG-63 cells. In summary, enrichment of WPI with PG may be a promising strategy to prevent microbial contamination while still promoting stem cell attachment and growth.

1. Introduction

Treatment of critical size bone defects generally requires surgeries involving implantation of autologous bone grafts or bone graft substitutes. Tissue engineering (TE) aims to develop innovative scaffolds for the regeneration of tissues. The approach of delivering stem cells to the defect site on scaffolds with osteoconductive properties to enhance bone healing has attracted great attention. The formation of new bone tissue depends on the osteogenic development of appropriate stem cells [1]. Besides the great efforts to treat large critical-sized bone defects, few clinical applications are available due to the limitations of materials and low functionality of the platforms [2]. Hydrogels possess great advantages in bone repair, as they composed of three-dimensional hydrophilic polymer chains, which have superior mechanical strength and can provide nutrient environments suitable for endogenous cell growth. They are able to mimic the natural ECM, thus presenting a prospective ability to encapsulate bioactive molecules or cells. Additionally, raw materials for preparation of hydrogels are extensive and readily available, and they can be tailored to obtain the desired geometry for implantation or injection, and the degradation rate and porosity can be easily controlled by altering the crosslinking method and degree.

Recent advances in tissue engineering have focused on novel multifunctional biomaterials [3] based on renewable resources of great natural abundance, low cost and safety for human health. Protein-based eco-friendly biomaterials such as dairy proteins are currently of interest as substitutes for commercial materials for biomedical applications [4].

* Correspondence to: T.E.L. Douglas, Engineering Department, Lancaster University, UK.
** Correspondence to: M. Chatzinikolaidou, Department of Materials Science and Technology, University of Crete, 70013 Heraklion, Greece.
E-mail addresses: t.douglas@lancaster.ac.uk (T.E.L. Douglas), mchatzin@materials.uoc.gr (M. Chatzinikolaidou).

Whey proteins represent 20% of total milk proteins and are generally generated as a by-product of cheese manufacture. They are unique from a nutritional point of view as they contain all the essential amino acids, and they contain β-lactoglobulin, α-lactalbumin, immunoglobulins and bovine serum albumin [5,6]. In addition, antimicrobial activity in milk is mainly attributed to some minor whey proteins such as lactoferrin, lysozyme, immunoglobulins, and lactoperoxidase [7,8].

Furthermore, WPI solutions can form hydrogels upon heating; an important practical advantage of WPI hydrogels is that they withstand sterilization by autoclaving, a commonly used and clinically accepted sterilization technique. Hydrogels display several advantages when compared to other materials used for TE, including solid polymer scaffolds and ceramic scaffolds: they are non-brittle and incorporation of biologically active substances is straightforward.

Polyphenols have been implicated as components of antimicrobial hydrogels [9,10]. Polyphenols are derived from plants and are known to possess antibacterial effects and antioxidative properties. This is beneficial in bone TE, as oxidative stress has been indicated to impede both the differentiation of osteoblasts and the resorption of bone by osteoclasts *in-vitro* [11,12]. The ability to ameliorate oxidative stress by phenolic compounds such as gallic acid isolated from terrestrial plants, and phloroglucinol (PG) found in seaweeds has been documented in numerous reports [13,14]. PG has also been found to inhibit metastatic ability of breast cancer cells *in vitro* and *in vivo* [15]. The antibacterial effect of phlorotannins, polyphenols derived from brown seaweed of which PG is the basic subunit, is well-known [16], while recent research suggests that PG in its different forms also possesses antimicrobial activity [17,18]. Healthcare-associated infections (HAI) are a burden worldwide, especially due to the increasing prevalence of antibiotic-resistant strains. Hence, antimicrobial activity is an added value for biomaterials used in TE applications.

Bone marrow (BM)-derived mesenchymal stem cells (MSCs) are the major cell source for bone TE. However, the morbidity of the donor site and painful procedures for harvesting these cells have limited their application [19]. Recently, human dental pulp stem cells (DPSCs) were introduced as an alternative to multipotent stem cells with self-renewal ability [20]. These cells could be harvested from both primary and permanent teeth during routine teeth extraction procedures in orthodontic treatment [20]. For bone TE, DPSCs showed a higher proliferative ability and number of colony clusters compared to BM-MSCs [21]. Although other sources of MSCs have been applied for the regeneration of hard tissues, the complications at the site of harvest have limited their applications in practice. The DPSCs are an easily accessible source of MSCs with similar characteristics to bone marrow-derived stem cells and therefore can be used for hard tissue regeneration [22]. Due to their availability and differentiation potential, the application of these cells for TE has attracted enormous attention in recent years, including bone TE studies in animal models [21–24].

MG-63 cells derived from human osteosarcoma have been widely used in bone biology research to assess the *in vitro* osteogenic potential of biomaterials for bone TE and the pharmacokinetics for bone disease, as an alternative to normal osteoblastic cells due to ease of their availability and reproducibility of experimental results [25,26]. MG-63 cells together with Saos2 and MC3T3-E1 cell lines are used as reliable and adequate cell culture models that resemble the behavior of primary osteoblasts. However, differences in phenotypic characteristics, proliferative capacity, secretion of osteogenic proteins and gene expression levels in MG-63 and osteoblasts have been reported, including the expression of abundant amounts of type III collagen and fibronectin in MG-63 cells [27]. The latter are constituents of soft connective tissue and absent in mineralized bone. Despite these differences, the MG-63 cell line is a useful cell model for *in vitro* biological assessment, including the evaluation of cell attachment, proliferation and osteogenic differentiation.

In this paper, DPSCs and MG-63 cells were cultured in the presence of WPI-PG hydrogels, namely WPI hydrogels modified with different concentrations of PG, and were evaluated for their viability, proliferation, cell adhesion, morphology, potential to enhance extracellular collagen production and antimicrobial properties. As this potential is expected to be different for cell lines and primary cells, physiological and cancer cell types, a comparative *in vitro* biocompatibility study was performed. Viability and proliferation of both cell types on the WPI hydrogels were quantified by means of the PrestoBlue® cell viability assay. Cell adhesion and morphology of both cell types on WPI-PG hydrogels were visualized by means of scanning electron microscopy (SEM). Moreover, the collagen levels in culture supernatants were determined as a marker of extracellular matrix (ECM) formation. Ten bacterial strains involved in healthcare associated infections (HAI), including Gram-positive and Gram-negative bacteria, were selected to perform sensitivity assays with WPI-PG hydrogels and evaluate their antimicrobial effects. All these strains present various types of primary and opportunistic HAI as well as food-born and environmental infections. Seven of these strains belong to species included in the recently published list of drug-resistant bacteria that pose great health threats [28].

2. Materials and methods

2.1. Hydrogel preparation

Stock solutions of 40% WPI (*w/v*) were prepared by dissolving 20 g of WPI powder in 50 ml of deionised H_2O. A sonicator was used to facilitate dissolution and minimize foaming. Subsequently, 15 ml of WPI stock solution was transferred to Falcon tubes, and the required amount of phloroglucinol (Sigma-Aldrich, Germany) was added. The WPI solutions enriched with 0 (control), 2.5, 5, 10 and 20% w/v PG concentrations are designated as WPI-PG-0%, WPI-PG-2.5%, WPI-PG-5%, WPI-PG-10%, and WPI-PG-20%, respectively (Table 1). The WPI-PG solutions were vortexed until mixed homogenously, and 15 ml were poured into 9 cm (in diameter) Petri dishes and autoclaved at 121 °C for 15 min to simultaneously sterilise and induce gelation. Samples were then cooled to 60 °C and cooled further at ambient temperature. The WPI-PG hydrogels were cut into disc-shaped samples by means of a biopsy punch with a diameter of 8 mm and a weight of approximately 50 mg.

2.2. Surface topography studies

Sample cross-sections comprising a range of WPI-PG hydrogels were viewed by SEM. SEM analysis was performed using a 7800F JEOL SEM instrument. Prior to SEM analysis, samples were mounted on aluminum stubs (Agar Scientific Ltd., UK) using carbon adhesive pads (Agar Scientific Ltd., UK) and coated with a 10 nm layer of gold using a Q150RES sputter coater (Quorum Technologies Ltd). SEM was used to analyze differences in the surface topography of WPI-hydrogels modified with PG concentrations ranging from 0 to 20%.

2.3. Mechanical testing

The effects of PG incorporation into WPI hydrogels on the hydrogels' mechanical properties were evaluated. Cylindrical WPI samples of 2.5, 5, 10 and 20% PG, measuring 10 mm in height and 8 mm in diameter,

Table 1
WPI hydrogels enhanced with different concentrations of PG. The WPI content of 40% (*w/v*) was the same for all WPI-PG hydrogels.

Material designation	PG content (%w/v)
WPI-PG-0% (control)	0
WPI-PG-2.5%	2.5
WPI-PG-5%	5
WPI-PG-10%	10
WPI-PG-20%	20

were subject to compressive testing using a Zwick 1435 Universal Testing Machine. Test parameters were set at a speed of 10 mm per minute, and a test range of 0–95% strain.

2.4. DPSCs and MG-63 cell culture maintenance

DPSCs cultures were established after generous donation by Prof. A. Bakopoulou at the School of Dentistry at the Aristotle University of Thessaloniki, Greece. Based on a previously described protocol [22], DPSCs cultures were established using an enzymatic dissociation method following their isolation from wisdom teeth of healthy donors after informed consent according to the Declaration of Helsinki (ethical approval number: 322/15-4-2013 by the Institutional Ethics Committee). Briefly, following disinfection of third molars, a cut was made around the cementum-enamel junction to expose the pulp chamber. Then, the pulp was retrieved, thoroughly minced and digested for 45 min at 37 °C with a mixture of 3 mg/ml of collagenase I and 4 mg/ml of dispase II (Invitrogen, Karlsruhe, Germany). DPSCs were cultured in minimum essential media α-MEM (Invitrogen) supplemented with 15% fetal bovine serum (FBS, Invitrogen), 100 mM L-ascorbic acid phosphate (Sigma-Aldrich, Steinheim, Germany), 100 units/ml of penicillin, 100 mg/ml of streptomycin and 1% amphotericin as previously described by the same team [22]. All experiments were conducted with DPSCs at passages 2 to 4.

The osteosarcoma cell line MG-63 was purchased from Sigma (USA) and cultivated in DMEM containing 100 units/ml of penicillin, 100 mg/ml of streptomycin and 1% amphotericin (all from Gibco), supplemented with 10% fetal bovine serum (FBS) according to bibliography [29–31]. Cells were maintained in a humidified atmosphere under 5% CO_2 at 37 °C, and the media were changed twice a week.

2.5. Cell viability and proliferation assay

The viability and proliferation of DPSCs and MG-63 on WPI-PG hydrogels was quantitatively assessed using the resazurin-based metabolic assay PrestoBlue® (Invitrogen, USA) as previously described [32]. Briefly, the disc-shaped WPI-PG scaffolds, generated by using an 8 mm biopsy cutter, were placed into 48-well plates and each sample was seeded with 2×10^4 cells. At each experimental time point of 2, 4 and 7 days of culture, the PrestoBlue® reagent was added directly to the wells at a 1:10 ratio in culture medium and incubated at 37 °C for 60 min, before measuring the absorbance at 570 and 600 nm in a spectrophotometer (Synergy HTX Multi-Mode Microplate Reader, BioTek, Winooski, VT, USA). Three independent experiments were performed in triplicate.

2.6. Adhesion and morphology of the DPSCs and MG-63 cells on the WPI-PG hydrogels

The adhesion and morphology of DPSCs and MG-63 osteoblast-like cells were observed using SEM (JEOL JSM-6390 LV) after 2, 4 and 7 days in culture. Seeded scaffolds with 2×10^4 cells per sample were placed in a CO_2 incubator at 37 °C for 2, 4 and 7 days and then were removed from the incubator and rinsed three times with PBS, fixed with 4% *v*/v paraformaldehyde for 20 min and dehydrated in increasing concentrations (30–100% *v*/v) of ethanol. The scaffolds were then dried in a critical point drier (Baltec CPD 030), sputter-coated with a 20 nm thick layer of gold (Baltec SCD 050) and observed under SEM at an accelerating voltage of 15 kV.

2.7. Determination of the produced extracellular collagen

A modified Sirius red assay [33] was used to stain total collagen produced in the extracellular matrix. The anionic dye Sirius Red binds to the [Gly–X–Y] tripeptide of mammalian cells. Collagen is a basic protein, and it is thus likely that the sulphonic groups of the dye may interact at low pH with the amino groups of lysine and hydroxylysine, and with the guanidine groups of arginine [34]. On days 2, 4 and 7 of the experiment, the culture supernatants were collected, and 25 μl were diluted to a final volume of 100 μl with ultrapure water. Then 1 ml of the dye solution consisting of 0.1% *w/v* Sirius red F3B (Sigma-Aldrich, St. Louis, MO, USA) in 0.5 M acetic acid was added, and the samples were incubated at room temperature for 30 min. The samples were centrifuged at 15,000*g* for 20 min to pellet the collagen–dye complex. The pellet was washed with 0.5 ml of 0.5 M acetic acid to remove the unbound dye. Dissolution of the collagen–dye complex with 1 ml of 0.5 M NaOH followed, and 200 μl of the solution were transferred into 96-well plates to measure the absorbance at 530 nm (Synergy HTX Multi-Mode Microplate Reader, BioTek, Winooski, VT, USA). Collagen concentration was determined by means of a calibration curve. Samples were analyzed in quadruplicate.

2.8. Microbiological assays

Bacterial strains used in the study included *Bacillus cereus* (MCIMB 9373), *Enterococcus faecalis* (NCTC 12697), *Escherichia coli* (NCTC 9001), *Klebsiella oxytoca* (ATCC 15764), *K. pneumoniae* (40602), *Pseudomonas aeruginosa* (NCTC 6749), *Staphylococcus aureus* (NCTC 6571), *S. aureus* (MRSA) [originated from NCTC 13552], *S. epidermidis* (NCTC 11047), *Streptococcus pyogenes* (NCIMB 8198).

For susceptibility testing, the bacterial strains were grown overnight on nutrient agar (Oxoid CM0003) at 37 °C. Inocula were prepared according to the standard protocol (Andrews and BSAC Working Party On Susceptibility Testing ft. 2001). Disc-shaped WPI—PG hydrogels were prepared and placed onto a bacterial inoculum. For sensitivity tests, the samples were placed on the surface of plates containing 25 ml of Isosensitest agar (Oxoid CM0471) or (in some experiments) nutrient agar. Before placing the samples, the agar plates were swabbed with microbial suspensions. The plates were incubated overnight at 37 °C. Zones of inhibition (ZOI) were recorded after 18–30 h when bacterial lawns became clearly visible on the agar.

To test modes of inhibition of bacterial growth, the samples of hydrogels were removed from ZOI using sterile forceps, and central areas of ZOI without any signs of bacterial growth were touched firmly a few times with sterile wet swabs, streaked out (in single lines) onto sectors on nutrient agar plates (Supplementary Fig. 2), and incubated overnight at 37 °C. The absence of bacterial growth on the streaked areas was interpreted as bactericidal inhibition; the restoration of growth indicated bacteriostatic effects.

2.9. Statistical analysis

The experimental data were analyzed using two-way ANOVA followed by Tukey's multiple comparisons test among groups. Data were expressed as means ± standard deviation (SD). For these analyses the GraphPad Prism software version 8.0 (La Jolla, USA) was used. The symbols * designate $p < 0.05$; ** $p < 0.01$; *** $p < 0.001$; **** $p < 0.0001$; ns denotes statistically non-significant differences.

3. Results

3.1. WPI-PG hydrogels and surface characterization by means of SEM

Sterile, disc-shaped WPI-PG hydrogels were prepared as described in Section 2.1, and based on their PG concentration they were denoted as WPI-PG-0% (control), WPI-PG-2.5%, WPI-PG-5%, WPI-PG-10%, and WPI-PG-20%. The WPI-PG hydrogels changed colour from yellowish for WPI-PG-0% to dark brown for the WPI-PG-2.5%, WPI-PG-5%, WPI-PG-10%, and WPI-PG-20% (Fig. 1).

The microstructures of WPI-PG hydrogels with concentrations ranging from 0 to 20% PG were analyzed *via* SEM (Fig. 2). The WPI control (0% PG) sample presented a consistently smooth surface topography. It is conceivable that the increase in roughness is caused by

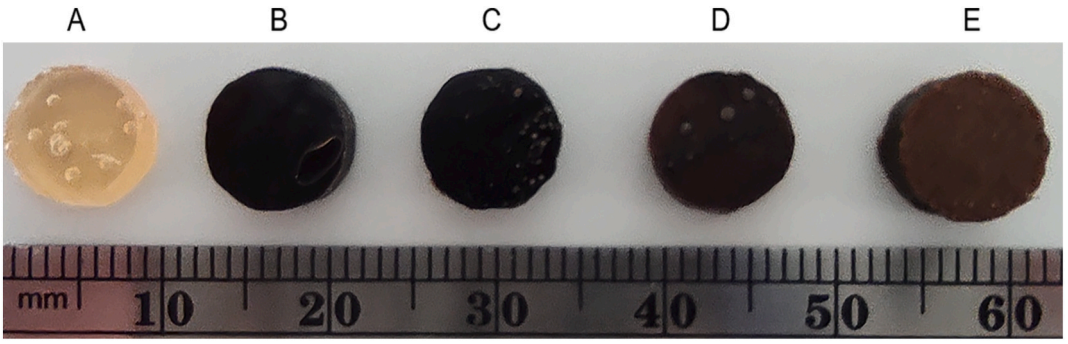

Fig. 1. Macroscopic images of disc-shaped samples prepared from hydrogels solidified and autoclaved in petri dishes. A: WPI-PG-0%, B: WPI-PG-2.5%, C: WPI-PG-5%, D: WPI-PG-10%, E: WPI-PG-20%.

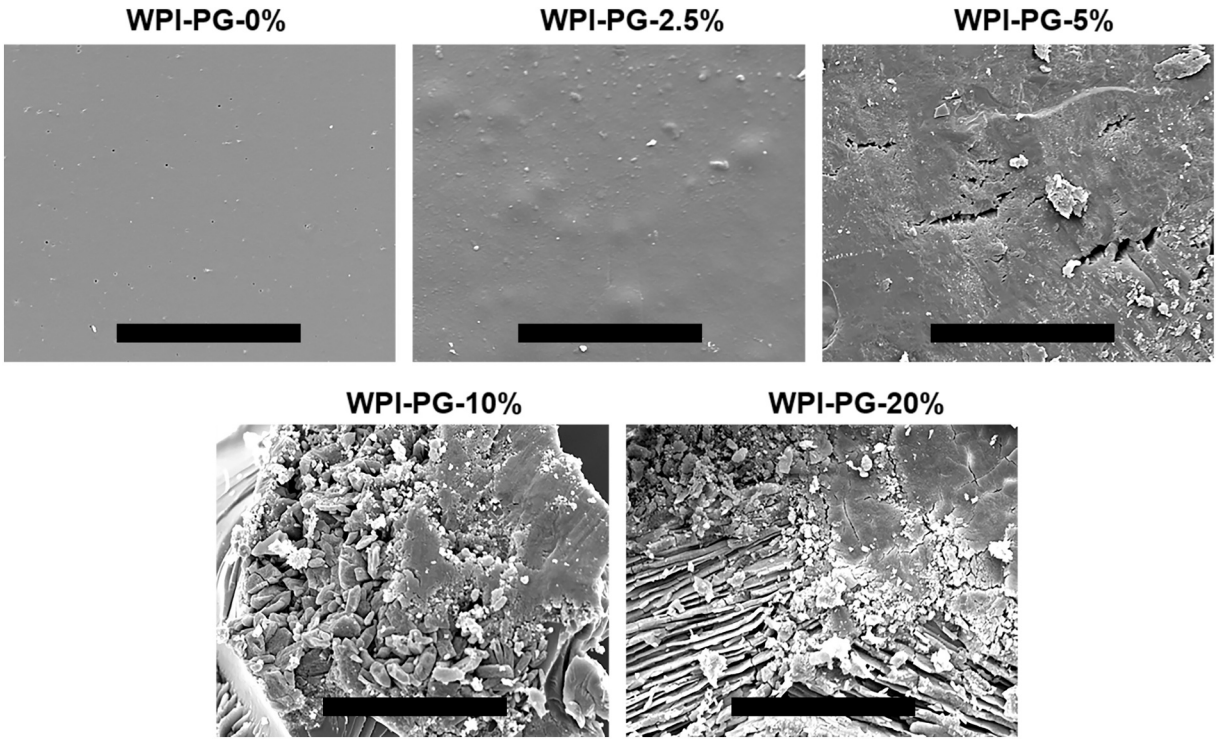

Fig. 2. SEM images displaying alterations in surface topography of WPI hydrogels containing PG at concentrations of 0%, 2.5%, 5%, 10% and 20%. Scale bars on SEM images indicate 100 μm.

the presence of PG in the hydrogel, which may form deposits when hydrogels are dried during preparation for SEM studies.

3.2. Mechanical testing

The WPI-PG-0%, WPI-PG-2.5%, WPI-PG-5%, WPI-PG-10% and WPI-PG-20% hydrogels were characterized for mechanical properties by measuring their compressive strength, Young's modulus and % strain at break (Fig. 3). It is important to note that, due to high friction caused by the nature of the samples, the WPI hydrogels supplemented with 20% PG became stuck in the jaws of the Zwick testing machine, meaning values for strength, modulus and strain at break may have been overestimated.

3.2.1. Compressive strength

The compressive strength values for WPI hydrogels containing 0, 2.5, 5, 10 and 20% PG are shown in Fig. 3A. No statistically significant difference in compressive strength was observed between the WPI control (0% PG) and the 2.5% PG sample group (mean values of 4.26 and 4.34 MPa, respectively). However, increasing the PG concentration to 5% resulted in the compressive strength decreasing by 1.35 MPa to a mean of 2.91 MPa. This reduction was deemed to be statistically insignificant compared to both the WPI control and the 2.5% PG sample group ($P < 0.05$). Increasing the PG concentration to 10% led to a mean compressive strength of 5.06 MPa. However, values were inconsistent within this group and no statistical significance was proven. Values for the 20% PG sample group were significantly higher by a factor of approximately three compared to the other groups; however, these values may have been overestimated.

3.2.2. Young's modulus

Except for the 20% PG sample group for which values may have been overestimated, no statistically significant difference in Young's modulus was observed between PG supplemented sample groups compared to the WPI control (Fig. 3B). The addition of 2.5% PG resulted in a negligible increase in Young's modulus, while 5% PG caused a negligible decrease. A statistically significant increase of 0.43 MPa was observed when PG concentration was increased from 5% to 10%. However, all samples

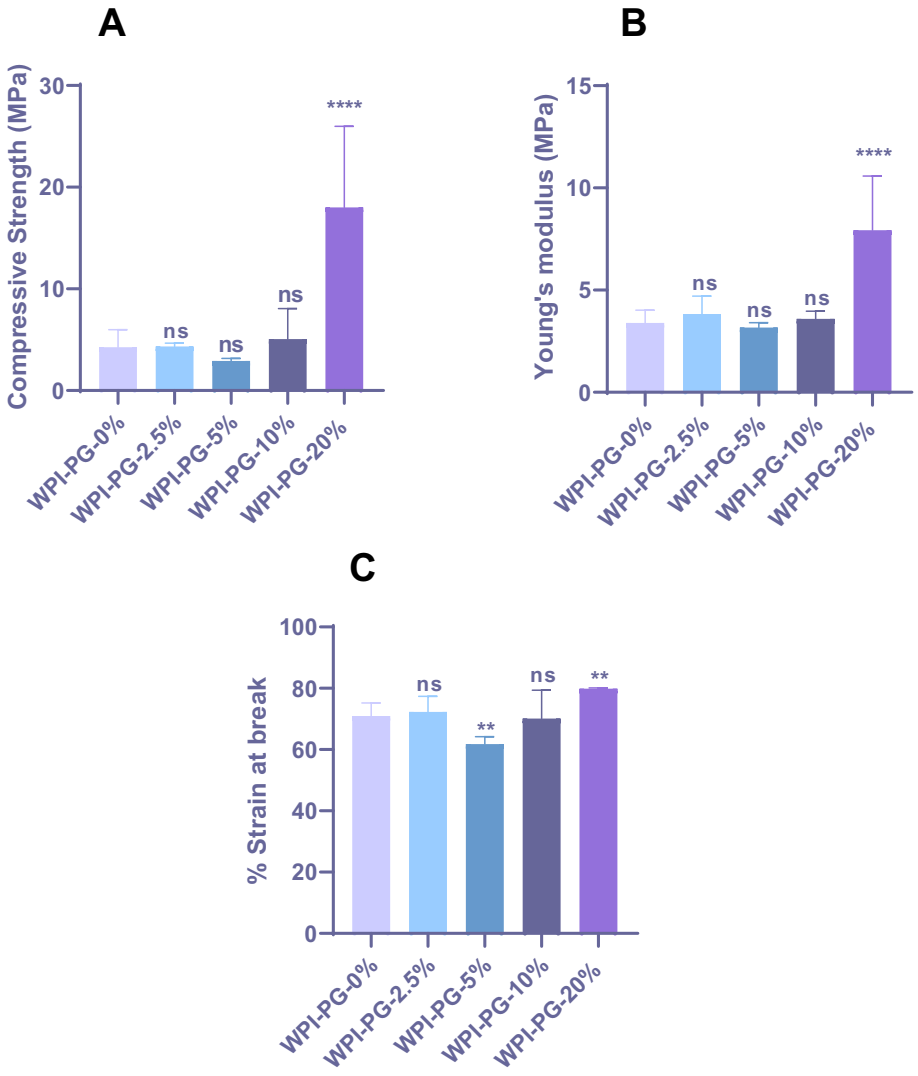

Fig. 3. Mechanical testing of WPI hydrogels containing 0, 2.5, 5, 10 and 20% PG. A: Compressive strength; B: Young's modulus; C: Strain at break. Each bar represents the mean ± SD of nine replicates (*p < 0.05, **$p < 0.01$, ****$p < 0.0001$; ns denotes statistically non-significant difference compared to the WPI-PG-0 control).

demonstrated a Young's modulus between 3 and 4 MPa.

3.2.3. *Strain at break*

The % strain at break of the WPI samples with different PG concentrations is presented in Fig. 3C. The mean deformation observed for the WPI control (0% PG) sample group was 7.09 mm (70.92%). The presence of 2.5% PG in WPI hydrogels resulted in a slight increase in the strain at break (72.31%) while supplementation of 10% decreased this value to 70.14%. However, except for the potential overestimate in the 20% PG samples, the only statistically significant difference ($p < 0.05$) observed for strain at break coincided with the addition of 5% PG (61.78%).

3.3. *Cell viability and proliferation*

Cellular viability and proliferation of DPSCs and MG-63 on WPI-PG-0%, WPI-PG-2.5%, WPI-PG-5%, WPI-PG-10% and WPI-PG-20% hydrogels were quantitatively assessed by measuring their metabolic activity after 2, 4 and 7 days in culture (Fig. 4). For the whole incubation period, cell numbers for both cell types investigated were found to be higher on the tissue culture treated polystyrene (TCPS) control than on the WPI-PG hydrogels (Fig. 4A, C).

DPSCs displayed increased metabolic activity, expressed as absorbance value, from day 4 to day 7 in all samples, with the WPI-PG-10% and WPI-PG-5% hydrogels demonstrating non-significant difference to TCPS control during day 4 (Fig. 4A). As compared with DPSCs, MG-63 osteosarcoma cells presented a decrease of metabolic activity from day 4 to day 7 in all samples, indicating a downregulated proliferation potential of osteosarcoma cells on WPI-PG hydrogels.

3.4. *Effects of WPI-PG hydrogels on cell adhesion, morphology and growth*

Representative SEM images show DPSCs on WPI-PG-0%, WPI-PG-2.5%, WPI-PG-5%, WPI-PG-10% and WPI-PG-20% hydrogels, 4 and 7 days post-seeding (Fig. 5). Images at days 4 and 7 showed cell spreading for increased PG concentrations in WPI-PG-10% and WPI-PG-20% hydrogels with DPSCs, however without displaying their characteristic spindle shape morphology until day 7. On day 7 in culture, DPSCs displayed cell-cell interactions that promote tissue formation. Cell infiltration within the pores of the WPI-PG-10% and WPI-PG-20% hydrogels was observed in Fig. 5. In contrast, MG-63 cells appear round on the surface of the hydrogels with an obvious decrease in cell density on WPI-PG-2.5% and WPI-PG-5% hydrogels (Fig. 6). On the latter two

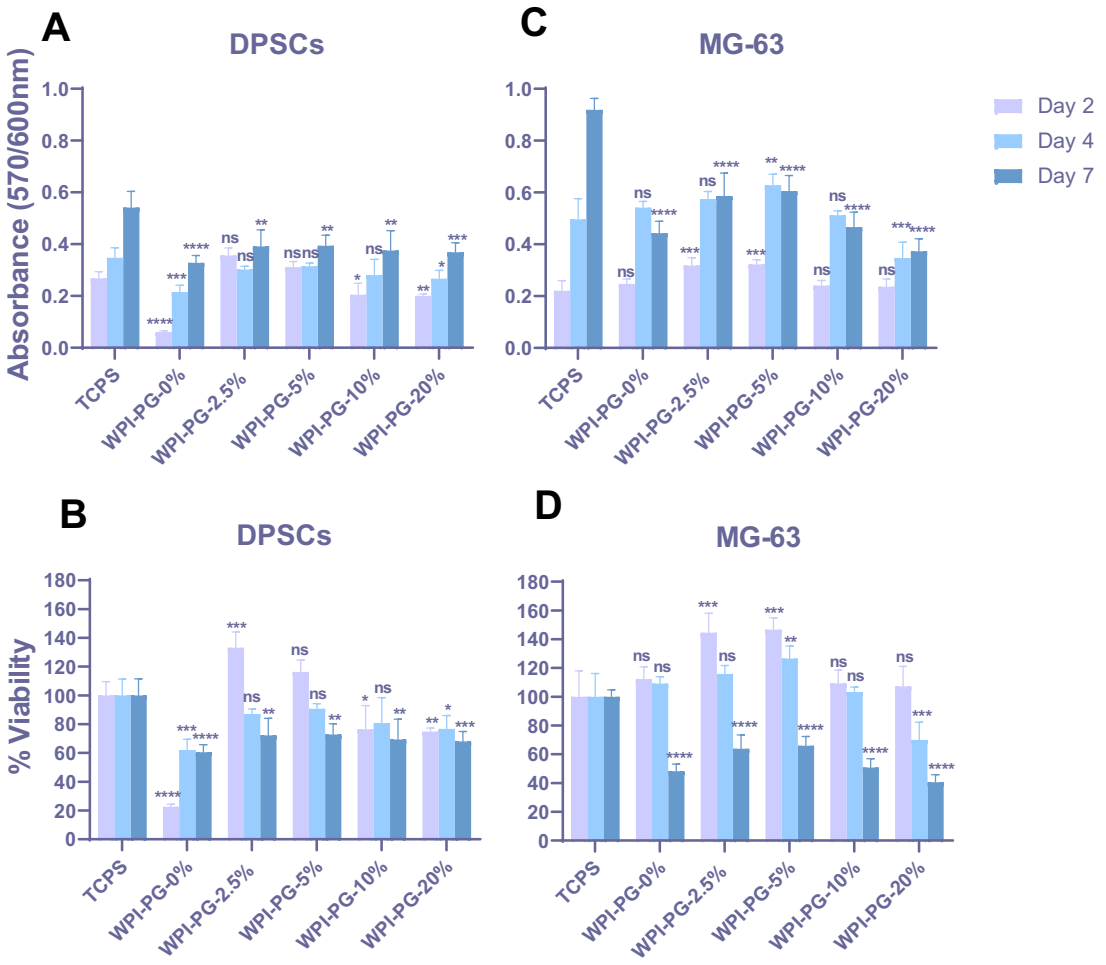

Fig. 4. Cell viability and proliferation of DPSCs (A, B) and MG-63 (C, D) cells cultured in the presence of WPI hydrogels with different PG concentrations, expressed as absorbance (A, C) and % viability of the TCPS control set at 100% for each experimental time point (B, D). Each bar represents the mean ± SD of quadruplicates (*$p < 0.05$, **$p < 0.01$, ***$p < 0.001$, ****$p < 0.0001$; ns denotes a statistically non-significant difference compared to the TCPS control at the corresponding time point).

compositions the observed cell density of DPSCs was lower as well.

The morphology of MG-63 cells on WPI-PG-0%, WPI-PG-2.5%, WPI-PG-5%, WPI-PG-10% and WPI-PG-20% hydrogels on day 4 and 7 was visualized *via* SEM and presented in Fig. 6. WPI-PG-10% and WPI-PG-20% hydrogels WPI-PG-10% promoted cell spreading.

3.5. Extracellular collagen production

In order to investigate the potential of ECM formation by DPSCs and MG-63 cultured on the WPI-PG hydrogels, the secretion of collagen was determined, as collagen constitutes the main structural element of the ECM. We quantified the total collagen secreted in culture supernatants at different time intervals, as shown in Fig. 7, in the presence of exogenous ascorbic acid which is a co-factor in collagen synthesis [35]. We found that DPSCs produced similar levels of collagen on days 2 and 4 in the presence of all WPI-PG hydrogels. On day 7, significantly lower values were observed for WPI-PG-2.5%, WPI-PG-5%, and WPI-PG-10% compared to the WPI-PG-0% control, while for WPI-PG-20% they were the highest among the hydrogels and similar to the control. MG-63 osteosarcoma cells exhibit significantly lower levels of collagen production compared to the DPSCs cultures. Collagen production levels in MG-63 cultures were similar to the WPI-PG-0% control on days 2 and 4, except of the WPI-PG-20% hydrogels that indicated significantly higher values than the control on day 2.

3.6. Antibacterial properties of WPI-PG hydrogels

First assays involving testing of antimicrobial properties of disc-shaped WPI-PG hydrogels were carried out against a MRSA strain. The examples of these experiments are shown in Supplementary Fig. 1. It is evident from Supplementary Fig. 1a that 5 mg of the WPI-PG-2.5%, WPI-PG-5% and WPI-PG-10% hydrogels did not inhibit the MRSA growth, but there was slight growth inhibition with a narrow ZOI in WPI-PG-20%. The assay involving 20 mg of WPI-PG-20% showed a clear ZOI. To enhance the assay sensitivity, the amount of the hydrogels was increased to 30 mg in the next experiment (Supplementary Fig. 1b), in which five bacterial species (*Pseudomonas aeruginosa*, *Staphylococcus epidermidis*, *Bacillus cereus*, *Escherichia coli* and *Streptococcus pyogenes*) manifested clear ZOI, and one species (*Enterococcus faecalis*) was marginally inhibited in its growth. These results suggest an obvious antibacterial potential of the hydrogel at least against seven bacterial species. Moreover, disc-shaped hydrogel samples were used for the sensitivity testing, and the results are shown in Fig. 8. All four bacterial species used in this experiment were clearly inhibited in their growth by WPI-PG hydrogels at all used concentrations of PG on two different media (Iso-sensitest and nutrient agar). The level of inhibition (ZOI size) was dependent on PG concentrations. Overall, the inhibitory effects were stronger and clearer on Iso-sensitest agar than on nutrient agar, although the results for *P. aeruginosa* were comparable on both media. The blank WPI hydrogels without PG did not manifest any inhibitory effects.

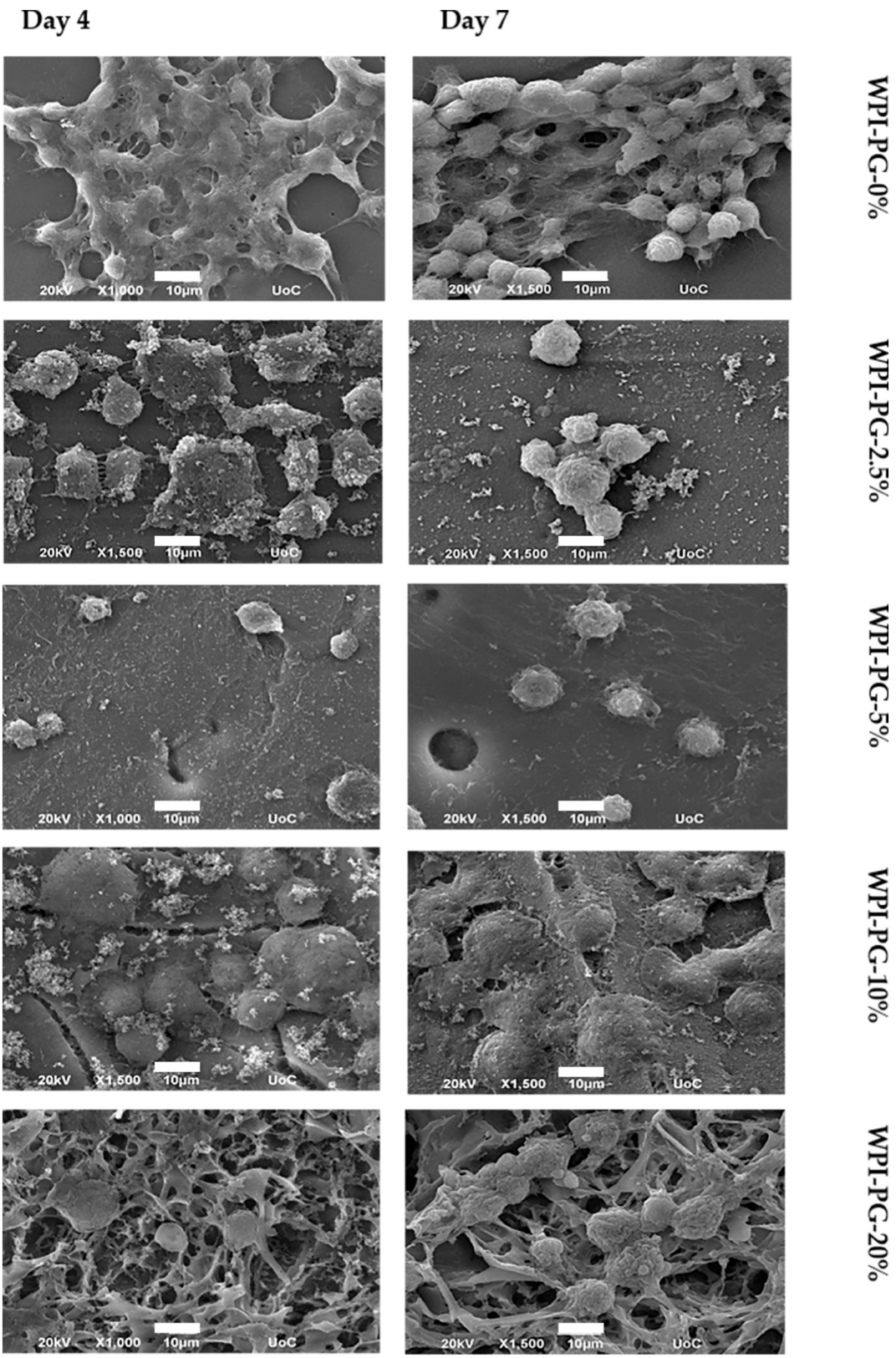

Fig. 5. Evaluation of cell attachment and morphology of DPSCs cultured on WPI hydrogels modified with different PG concentrations after 4 and 7 days in culture. Scale bars represent 10 µm.

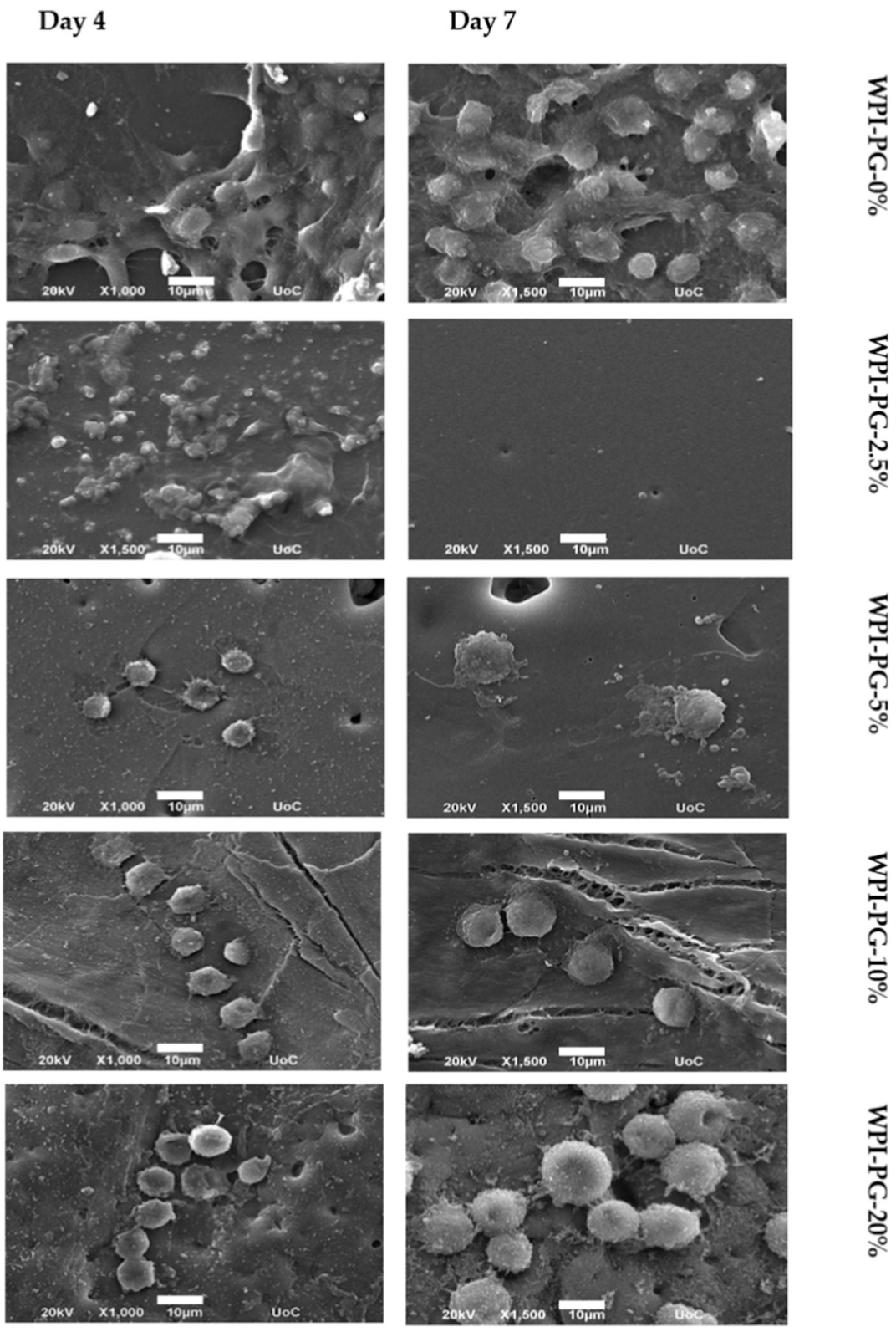

Fig. 6. Evaluation of cell attachment and morphology of MG-63 osteosarcoma cells cultured on WPI hydrogels modified with different PG concentrations, after 4 and 7 days in culture. Scale bars represent 10 μm.

After recording the results on sensitivity testing (next day following swabbing), we reused the plates with ZOI for determining the mode of growth inhibition in a simple assay (see Methods). Supplementary Fig. 2 shows an example of results from such assay performed for WPI-PG-10% and WPI-PG-20% hydrogels within the experiment depicted in Fig. 8. The mode of inhibition depended on PG concentrations and media used. Bactericidal growth inhibition was observed for WPI-PG-20% hydrogels in *P. aeruginosa* on both media, and in *S. epidermidis* on Iso-sensitest, as well as for WPI-PG-10% hydrogels in *S. epidermidis* on Iso-sensitest. Predominantly bactericidal inhibition with a bacteriostatic effect for a

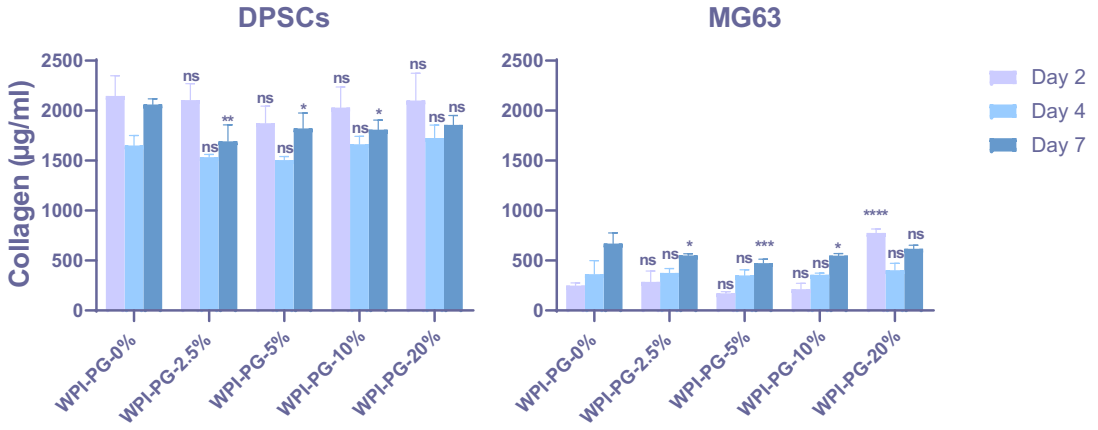

Fig. 7. Levels of total collagen in the supernatants of the DPSCs (left) and the MG-63 cells (right) cultured on the different PG concentrations in WPI-hydrogels for 2, 4 and 7 days. Error bars represent the average of quadruplicates (*$p < 0.05$, **$p < 0.01$, ***$p < 0.001$, ****$p < 0.0001$; ns denotes statistically non-significant difference compared to the WPI-PG-0% control at the corresponding time point).

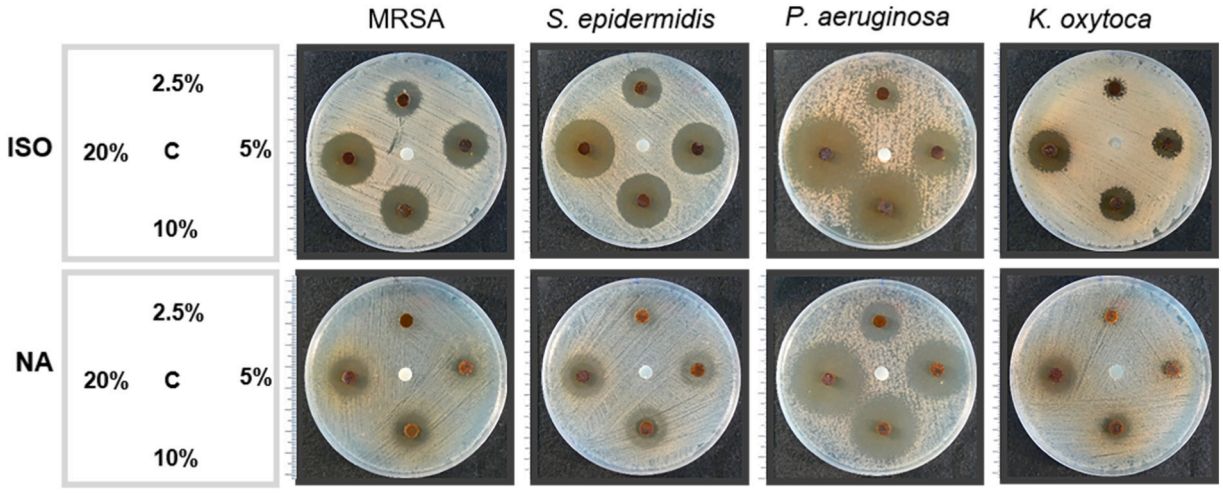

Fig. 8. Inhibition of bacterial growth by WPI-PG hydrogels on Iso-sensitest agar (ISO) and nutrient agar (NA). The squares on the left show the arrangement of hydrogel discs with different concentrations of PG and without PG (C). The ruler (with 1 mm scale) is attached to the left side of each image. The diameter of each plate is 9 cm.

low proportion of cells was observed for WPI-PG-20% hydrogels in MRSA on both media, and in *K. oxytoca* on nutrient agar. WPI-PG-10% hydrogels showed bacteriostatic inhibition on both media for MRSA, *K. oxytoca* and *P. aeruginosa*. Bacteriostatic inhibition was also observed for WPI-PG-20% hydrogels in *K. oxytoca* on Iso-sensitest, and in *S. epidermidis* on nutrient agar.

4. Discussion

Recent advances in TE focus on finding more biocompatible, biodegradable and non-toxic biomaterials with the ability to mimic the natural physiological environment and favor enhanced cell-material interactions. Protein-based biomaterials have the characteristics of improved bioresorbability, biocompatibility, tissue healing, and ability to promote regeneration [4,36–38]. In this work we report on WPI and PG for the development of multifunctional biomaterials for biomedical applications. PG was identified as a component of hydrogels due to its known antimicrobial and antioxidative properties. The investigation of biomaterials suitability for bone TE includes their capacity to promote cell proliferation, adhesion and ECM formation. We demonstrated that DPSCs and MG-63 showed different cellular responses when seeded on different WPI-PG hydrogels, which is in agreement with literature reports [25].

The microstructure of WPI hydrogels has been examined by means of SEM. As expected, the control WPI hydrogels (0% PG) displayed a homogenously smooth surface topography in the dry state [6]. With increasing PG concentration, hydrogels were observably rougher in the dry state. This may be an advantage for their potential applications in bone TE, as both stiffer [39] and rougher [40] surfaces are known to promote the differentiation of cells towards the osteoblastic phenotype.

Minimal increases in both Young's modulus and percentage strain at break were found in hydrogels supplemented with PG at lower concentrations of 2.5%. Since stiffer surfaces are known to promote the differentiation of cells towards the osteoblastic phenotype, PG imparted stiffness would improve the compatibility of these hydrogels with bone tissue. However, this effect was not observed in a dose-dependent manner. The values for Young's modulus, compressive strength and percentage strain at break remained relatively consistent throughout sample groups, even when the concentration of PG was increased to 10%. This suggests that the incorporation of PG into the WPI hydrogels has no significant impact on the overall structural function of WPI hydrogels up to a PG concentration of 10%. Values for hydrogels containing 20% PG were higher; however, it is important to note that, due to high friction, the WPI hydrogels supplemented with 20% PG remained

stuck in the jaws of the testing machine, and therefore it cannot be concluded that this PG concentration improves the aforementioned mechanical properties. As such, PG supplementation at higher concentration may alter the mechanical properties of WPI composites, resulting in 'stickier' hydrogels. In future work, one might consider strategies to reduce adhesion between samples and the testing machine jaws with minimal influence on mechanical properties, for example the insertion of a thin, non-adhesive piece of material between the jaws and the sample.

Discussion of the mechanisms for the effect (or lack of effect) of PG on WPI hydrogels' mechanical properties must remain speculative in view of the limited data available. It is known that phlorotannins interact with proteins, resulting in a dark brown colour [41], which was ascribed to non-covalent protein-phlorotannin interactions. One may expect similar interactions between proteins and PG, the fundamental subunit of phlorotannins, which would explain the brown colour observed in this study (Fig. 1). Possibly, the number of crosslinks caused by interactions between WPI proteins and PG must exceed a certain number in order to markedly influence mechanical properties. The increased "stickiness" of hydrogels containing 20% PG might be due to interactions between PG bound to the WPI hydrogel network and surfaces; hydrogels containing polyphenol groups have exhibited increased adhesiveness [42]. Again, one can speculate that a certain PG concentration should be exceeded before such "stickiness" becomes appreciable. Alternatively, it is possible that at high PG concentrations, some PG may have "precipitated" as particles within the hydrogels after cooling, which might conceivably cause mechanical reinforcement. However, as already mentioned, such discussion must remain speculative.

Since materials for biomedical applications are potential sites for exogenous and endogenous infections, it is beneficial if they possess antimicrobial properties [43]. To evaluate them, we used a simple and convenient approach of making disc-shaped hydrogel samples allowing easy standardization of weight, volume, shape and application of hydrogel materials to microbial inocula. These advantages of disc-shaped samples make them comparable in efficiency to paper discs used routinely in sensitivity assays involving liquids [44,45]. Using these samples allows quantification of sensitivity data (Supplementary Fig. 3).

Overall, all ten Gram-positive and Gram-negative bacteria used in our study were inhibited (in bactericidal or bacteriostatic mode) by WPI-PG hydrogels, suggesting presumably non-specific inhibitory mechanisms. Interestingly, *Candida albicans* was not inhibited by WPI-PG hydrogels (as shown in Supplementary Fig. 4), suggesting that eukaryotic cells might be generally tolerant to PG, which is consistent with our results for human cells cultivated *in vitro*. Modes of inhibition were determined by using a simple "streak out assay" to check re-growth of inhibited bacterial cells taken directly from ZOI. This assay is convenient and rapid. Although WPI itself possesses antimicrobial properties [46], we never observed inhibition of bacterial growth by WPI hydrogels without PG, probably due to the denaturation of proteins during hydrogels formation.

Ideally, an antibacterial biomaterial would exhibit both a burst release to prevent microbial colonization and help the recipient's cells win the "race to the surface", and also a prolonged release to prevent later microbial colonization. For this, more detailed studies of PG release are necessary in future work. In addition, testing of antimicrobial properties of samples after incubation in biological fluids for a more extended period of time would be prudent to verify the mid- to long-term antimicrobial activity.

Regarding the cell viability assessment of the DPSCs and MG-63 cells on the WPI-PG hydrogels, we quantitatively evaluated the cytotoxic effect of substrates according to ISO 10993-5, in which it is stated that reduction of cell viability by more than 30% is considered a cytotoxic effect. In accordance, no cytotoxic effect was observed on days 2 and 4 for both cell types that displayed viability rates from 87 to 145% compared to the TCPS control, with higher values on WPI-PG-2.5% and WPI-PG-5% hydrogels on day 2. On day 7, the cell viability for DPSCs ranged from 60% to 73% compared to the control, while MG-63 cells presented viability values from 40% to 65%. Increased PG concentrations led to an inhibition of the MG-63 proliferation, consistent with the previously reported anti-cancer activity of PG [13,15].

Collagen is the most abundant fibrous protein within the interstitial ECM that constitutes up to 30% of the total protein mass in mammals, providing tensile strength, regulating cell adhesion, supporting chemotaxis and migration, and directing tissue development [47]. Deposition of type I collagen-rich ECM is a prerequisite for the expression of specific osteoblast products, such as alkaline phosphatase, during the normal developmental sequence of the osteoblast [48]. Collagen levels secreted by DPSCs cultured on WPI-PG hydrogels are increased two to three-fold compared to the MG-63 secretion levels. These results suggest that WPI-PG hydrogels may have supported the ECM formation when seeded with DPSCs.

SEM micrographs of the 2D WPI-PG hydrogel surface underline the relationship between the increasing concentration of PG in the hydrogel and the supported adhesion and proliferation of DPSCs and MG-63 cells. In addition to cell adhesion, the morphology of the cells was evaluated. MG-63 osteosarcoma cells exhibited a round shape morphology in contrast to DPSCs, which were found to form cell-cell and cell-material interactions after 4 and 7 days in culture. Although MG-63 cells are widely used for biochemical studies of osteoblast-specific functions *in vitro*, their abundant type III collagen synthesis has been known to be unusual compared to other osteoblast lineages [49]. MG-63 osteosarcoma cells have been characterized as an atypical bone-forming model since the gene expression profile and the capability to synthesize a correct extracellular bone matrix are impaired [50]. It is also possible that the tumorigenic nature of MG-63 prevents them from properly adhering onto the WPI-PG hydrogels. In addition, the DPSCs culture contained ascorbic acid, a required cofactor for enzymes to hydroxylate proline and lysine in pro-collagen, enabling the collagen chains to form a proper helical structure [51]. The role of ascorbic acid in osteogenic differentiation is mainly attributed to the secretion of type I collagen into the ECM. The significantly higher total collagen production found in DPSCs cultures on WPI-PG hydrogels compared to the MG-63 cells is in line with the cell-cell interactions observed for DPSCs by means of SEM indicating good adhesion and a high affinity to the substrate, similar to a previous study displaying strong attachment of DPSCs onto chitosan/gelatin scaffolds that enhanced bone tissue formation *in vitro* and *in vivo* [22]. The presence of cell-cell interactions suggests active cell motility, which is essential for tissue formation within a scaffold, and this is in agreement with a recent report on dense ECM formation by DPSCs cultured onto biopolymer-based hydrogels that promoted the osteogenic response *in vitro* [52]. Another study towards bone TE demonstrated the capacity of DPSCs to strongly attach on antibacterial thymol-functionalized hybrid scaffolds, increasing proliferation and calcium mineralization [3]. Our findings reveal distinct advantages of WPI-PG hydrogels as multifunctional scaffolds for tissue engineering, as they support stem cell adhesion, extracellular matrix formation, inhibition of cancer cell growth and adhesion, and, importantly, they possess antibacterial properties. The exploration of the use of WPI-PG hydrogels in bone tissue engineering would necessitate more experimental data on the *in vitro* and *in vivo* osteogenic potential of these materials.

It was observed that the proliferation and viability of MG63 cells were lower at the highest concentrations of PG (10%, 20%), which also showed their highest antimicrobial activity. It is possible that one must strike a balance between antimicrobial activity and cell proliferation and viability. Interestingly, the reduction in proliferation and viability was not as pronounced for DPSCs. It may be speculated that MG63 cells, being osteocarcoma-derived, are more susceptible to the anticancer effect of PG, which has been reported previously for phlorotannins, of which PG is the fundamental subunit [53]. This study underlines the suitability WPI hydrogels as scaffolds for regeneration of bone tissue, as

bone-forming cells were able to grow on WPI hydrogels, as in previous studies [6,38]. Other authors have developed hydrogels for bone regeneration, both injectable and pre-formed, incorporating a mineral phase to combine the benefits of a hydrogel and a ceramic phase [54]. The WPI hydrogels in this study are pre-formed, and hence non-injectable, but they displayed values of Young's modulus of between 3 and 4 MPa (Fig. 3), which is considerably higher than values described for injectable hydrogels; for example, hydrogels of catechol/poly (ethylene glycol) (cPEG) and oligo[poly(ethylene glycol) fumarate] (OPF) used in previous work displayed Young's modulus values two orders of magnitude lower [55]. Stiffer surfaces are known to promote differentiation of cells towards the osteoblastic phenotype [56,57]. Future work may focus on the incorporation of a mineral phase into WPI-PG hydrogels to exploit the positive biological effects of PG described in this study.

5. Conclusions

In this study, WPI hydrogels were enriched with PG at concentrations of 0, 2.5, 5, 10 and 20% (*w/v*). Incorporation of PG into WPI hydrogels increased the solubilization of PG. The addition of PG into the WPI hydrogels did not lead to any decrease of the mechanical properties as evidenced by the compressive strength, Young's modulus and % strain at break. The WPI-PG hydrogels demonstrated antimicrobial activities against a range of bacteria causing common HAI. WPI-PG hydrogels supported the growth and collagen production of DPSCs for the formation of the extracellular matrix. Overall, WPI modification with PG supported mesenchymal stem cell adhesion and growth, inhibited cancer cell growth and adhesion, demonstrating a bactericidal and bacteriostatic inhibition of a range of pathogenic bacteria, thus presenting a promising strategy in the development of multifunctional biomaterials for tissue engineering.

Declaration of competing interest

The authors declare that they have no known competing financial interests or personal relationships that could have appeared to influence the work reported in this paper.

Acknowledgements

The research project was supported by the Hellenic Foundation for Research and Innovation (H.F.R.I.) under the “First Call for H.F.R.I. Research Projects to support Faculty members and Researchers and the procurement of high-cost research equipment grant” project number HFRI-FM17-1999.

T.E.L.D. thanks N8 Agrifood for financial support in the framework of the pump priming grant “Food2Bone”. Kristen Apostol is thanked for assistance in preparing WPI-PG hydrogels.

The authors acknowledge Ms. Stefanos Papadakis for expert technical assistance with SEM.

Appendix A. Supplementary data

Supplementary data to this article can be found online at https://doi.org/10.1016/j.msec.2021.112412.

References

[1] F. Shang, Y. Yu, S. Liu, L. Ming, Y. Zhang, Z. Zhou, J. Zhao, Y. Jin, Advancing application of mesenchymal stem cell-based bone tissue regeneration, Bioact. Mater. 6 (3) (2021) 666–683.

[2] S.N. Gorodzha, A.R. Muslimov, D.S. Syromotina, A.S. Timin, N.Y. Tcvetkov, K. V. Lepik, A.V. Petrova, M.A. Surmeneva, D.A. Gorin, G.B. Sukhorukov, R. A. Surmenev, A comparison study between electrospun polycaprolactone and piezoelectric poly(3-hydroxybutyrate-co-3-hydroxyvalerate) scaffolds for bone tissue engineering, Colloid Surf. B 160 (2017) 48–59.

[3] K. Parkatzidis, M. Chatzinikolaidou, E. Koufakis, M. Kaliva, M. Farsari, M. Vamvakaki, Multi-photon polymerization of bio-inspired, thymol-functionalized hybrid materials with biocompatible and antimicrobial activity, Polym. Chem. 11 (25) (2020) 4078–4083.

[4] T.E.L. Douglas, M. Vandrovcová, N. Kročilová, J.K. Keppler, J. Zárubová, A. G. Skirtach, L. Bačáková, Application of whey protein isolate in bone regeneration: effects on growth and osteogenic differentiation of bone-forming cells, J. Dairy Sci. 101 (1) (2018) 28–36.

[5] R.J.S. de Castro, M.A.F. Domingues, A. Ohara, P.K. Okuro, J.G. dos Santos, R. P. Brexó, H.H. Sato, Whey protein as a key component in food systems: physicochemical properties, production technologies and applications, Food Struct. 14 (2017) 17–29.

[6] D. Gupta, M. Kocot, A.M. Tryba, A. Serafim, I.C. Stancu, Z. Jaegermann, E. Pamuła, G.C. Reilly, T.E.L. Douglas, Novel naturally derived whey protein isolate and aragonite biocomposite hydrogels have potential for bone regeneration, Mater. Des. 188 (2020), 108408.

[7] A. Baldi, P. Ioannis, P. Chiara, F. Eleonora, C. Roubini, D.O. Vittorio, Biological effects of milk proteins and their peptides with emphasis on those related to the gastrointestinal ecosystem, J. Dairy Res. 72 (S1) (2005) 66–72.

[8] K. Yamauchi, H. Wakabayashi, K. Shin, M. Takase, Bovine lactoferrin: benefits and mechanism of action against infections. This paper is one of a selection of papers published in this Special Issue, entitled 7th International Conference on Lactoferrin: Structure, Functions, and Applications, and has undergone the Journal's usual peer review process, Biochem. Cell Biol. 84 (3) (2006) 291–296.

[9] H. Hashemi Gahruie, M. Niakousari, Antioxidant, antimicrobial, cell viability and enzymatic inhibitory of antioxidant polymers as biological macromolecules, Int. J. Biol. Macromol. 104 (Pt A) (2017) 606–617.

[10] C.J.H.J. Geng Huimin, Mussel-inspired hydrogels for tissue healing, Acta Chim. Sin. 78 (2) (2020) 105–113.

[11] B.E. Bax, A.S.M.T. Alam, B. Banerji, C.M.R. Bax, P.J.R. Bevis, C.R. Stevens, B. S. Moonga, D.R. Blake, M. Zaidi, Stimulation of osteoclastic bone resorption by hydrogen peroxide, Biochem. Biophys. Res. Commun. 183 (3) (1992) 1153–1158.

[12] N. Mody, F. Parhami, T.A. Sarafian, L.L. Demer, Oxidative stress modulates osteoblastic differentiation of vascular and bone cells, Free Radic. Biol. Med. 31 (4) (2001) 509–519.

[13] K.H. Kim, E. Moon, H.K. Kim, J.Y. Oh, S.Y. Kim, S.U. Choi, K.R. Lee, Phenolic constituents from the rhizomes of Acorus gramineus and their biological evaluation on antitumor and anti-inflammatory activities, Bioorg. Med. Chem. Lett. 22 (19) (2012) 6155–6159.

[14] S. Umadevi, V. Gopi, S.P. Simna, A. Parthasarathy, S.M. Yousuf, V. Elangovan, Studies on the cardioprotective role of gallic acid against AGE-induced cell proliferation and oxidative stress in H9C2 (2-1) cells, Cardiovasc. Toxicol. 12 (4) (2012) 304–311.

[15] R.K. Kim, Y. Suh, K.C. Yoo, Y.H. Cui, E. Hwang, H.J. Kim, J.S. Kang, M.J. Kim, Y. Y. Lee, S.J. Lee, Phloroglucinol suppresses metastatic ability of breast cancer cells by inhibition of epithelial-mesenchymal cell transition, Cancer Sci. 106 (1) (2015) 94–101.

[16] K. Nagayama, Y. Iwamura, T. Shibata, I. Hirayama, T. Nakamura, Bactericidal activity of phlorotannins from the brown alga Ecklonia kurome, J. Antimicrob. Chemother. 50 (6) (2002) 889–893.

[17] M. Chen, J.-Q. Cao, W.-J. Wang, N.-P. Li, Y. Wu, L. Wang, W.-C. Ye, Four new phloroglucinol-terpene adducts from the leaves of Myrciaria cauliflora, Nat. Prod. Bioprospect. 11 (1) (2021) 111–118.

[18] N. Khan, S. Rasool, S. Ali Khan, S. Bahadar Khan, A new antibacterial dibenzofuran-type phloroglucinol from Myrtus communis Linn, Nat. Prod. Res. 34 (22) (2020) 3199–3204.

[19] E.M. Bueno, J. Glowacki, Cell-free and cell-based approaches for bone regeneration, Nat. Rev. Rheumatol. 5 (12) (2009) 685–697.

[20] S. Gronthos, M. Mankani, J. Brahim, P.G. Robey, S. Shi, Postnatal human dental pulp stem cells (DPSCs) in vitro and in vivo, Proc. Natl. Acad. Sci. 97 (25) (2000) 13625–13630.

[21] M. Nakashima, K. Iohara, M. Murakami, Dental pulp stem cells and regeneration, Endod. Top. 28 (1) (2013) 38–50.

[22] A. Bakopoulou, A. Georgopoulou, I. Grivas, C. Bekiari, O. Prymak, K. Loza, M. Epple, G.C. Papadopoulos, P. Koidis, M. Chatzinikolaidou, Dental pulp stem cells in chitosan/gelatin scaffolds for enhanced orofacial bone regeneration, Dent. Mater. 35 (2) (2019) 310–327.

[23] Y. Fujii, Y. Kawase-Koga, H. Hojo, F. Yano, M. Sato, U.-i. Chung, S. Ohba, D. Chikazu, Bone regeneration by human dental pulp stem cells using a helioxanthin derivative and cell-sheet technology, Stem Cell Res Ther 9 (1) (2018) 24.

[24] G. Vagropoulou, M. Trentsiou, A. Georgopoulou, E. Papachristou, O. Prymak, A. Kritis, M. Epple, M. Chatzinikolaidou, A. Bakopoulou, P. Koidis, Hybrid chitosan/gelatin/nanohydroxyapatite scaffolds promote odontogenic differentiation of dental pulp stem cells and in vitro biomineralization, Dent. Mater. 37 (1) (2021) E23–E36.

[25] E.M. Czekanska, M.J. Stoddart, J.R. Ralphs, R.G. Richards, J.S. Hayes, A phenotypic comparison of osteoblast cell lines versus human primary osteoblasts for biomaterials testing, J. Biomed. Mater. Res. A 102 (8) (2014) 2636–2643.

[26] J. Clover, M. Gowen, Are MG-63 and HOS TE85 human osteosarcoma cell lines representative models of the osteoblastic phenotype? Bone 15 (6) (1994) 585–591.

[27] R.T. Franceschi, P.R. Romano, K.Y. Park, Regulation of type I collagen synthesis by 1,25-dihydroxyvitamin D3 in human osteosarcoma cells, J. Biol. Chem. 263 (35) (1988) 18938–18945.

[28] C. Willyard, Drug-resistant bacteria ranked, Nature 543 (7643) (2017) 15.

[29] F. Heshmatpour, S. Haghbin, Nanohydroxyapatite/graphene oxide nanocomposites modified with synthetic polymers: promising materials for bone tissue engineering applications, Int. J. Polym. Mater. Polym. Biomater. 70 (8) (2021) 585–591.
[30] G. Sharmila, C. Muthukumaran, S. Kirthika, S. Keerthana, N.M. Kumar, J. Jeyanthi, Fabrication and characterization of Spinacia oleracea extract incorporated alginate/carboxymethyl cellulose microporous scaffold for bone tissue engineering, Int. J. Biol. Macromol. 156 (2020) 430–437.
[31] Y.P. Singh, S. Dasgupta, S. Nayar, R. Bhaskar, Optimization of electrospinning process & parameters for producing defect-free chitosan/polyethylene oxide nanofibers for bone tissue engineering, J. Biomater. Sci. Polym. Ed. 31 (6) (2020) 781–803.
[32] A. Georgopoulou, M. Kaliva, M. Vamvakaki, M. Chatzinikolaidou, Osteogenic potential of pre-osteoblastic cells on a chitosan-graft-polycaprolactone copolymer, Materials (Basel, Switzerland) 11 (4) (2018) 490.
[33] C. Hadjicharalambous, E. Mygdali, O. Prymak, A. Buyakov, S. Kulkov, M. Chatzinikolaidou, Proliferation and osteogenic response of MC3T3-E1 pre-osteoblastic cells on porous zirconia ceramics stabilized with magnesia or yttria, J. Biomed. Mater. Res. A 103 (11) (2015) 3612–3624.
[34] N.R. Davis, O.M. Risen, G.A. Pringle, Stable, nonreducible cross-links of mature collagen, Biochemistry 14 (9) (1975) 2031–2036.
[35] F. Langenbach, J. Handschel, Effects of dexamethasone, ascorbic acid and β-glycerophosphate on the osteogenic differentiation of stem cells in vitro, Stem Cell Res Ther 4 (5) (2013) 117.
[36] J.E. Puskas, Y. Chen, Biomedical application of commercial polymers and novel polyisobutylene-based thermoplastic elastomers for soft tissue replacement, Biomacromolecules 5 (4) (2004) 1141–1154.
[37] M. Rouabhia, V. Gilbert, H. Wang, M. Subirade, In vivo evaluation of whey protein-based biofilms as scaffolds for cutaneous cell cultures and biomedical applications, Biomed. Mater. 2 (1) (2007) S38–S44.
[38] M. Dziadek, R. Kudlackova, A. Zima, A. Slosarczyk, M. Ziabka, P. Jelen, S. Shkarina, A. Cecilia, M. Zuber, T. Baumbach, M.A. Surmeneva, R.A. Surmenev, L. Bacakova, K. Cholewa-Kowalska, T.E.L. Douglas, Novel multicomponent organic-inorganic WPI/gelatin/CaP hydrogel composites for bone tissue engineering, J. Biomed. Mater. Res. A 107 (11) (2019) 2479–2491.
[39] A.S. Rowlands, P.A. George, J.J. Cooper-White, Directing osteogenic and myogenic differentiation of MSCs: interplay of stiffness and adhesive ligand presentation, *Am. J. Physiol. Cell Physiol.* 295 (4) (2008) C1037–C1044.
[40] S. Lossdorfer, Z. Schwartz, B.D. Boyan, Microrough implant surface topographies increase osteogenesis by reducing osteoclast formation and activity, J. Dent. Res. 82 (2003) B45.
[41] T.E. Douglas, A. Dokupil, K. Reczyńska, G. Brackman, M. Krok-Borkowicz, J. K. Keppler, M. Božič, P. Van Der Voort, K. Pietryga, S.K. Samal, L. Balcaen, J. van den Bulcke, J. Van Acker, F. Vanhaecke, K. Schwarz, T. Coenye, E. Pamuła, Enrichment of enzymatically mineralized gellan gum hydrogels with phlorotannin-rich Ecklonia cava extract Seanol(®) to endow antibacterial properties and promote mineralization, Biomed. Mater. (Bristol, England) 11 (4) (2016), 045015.
[42] B.P. Lee, P.B. Messersmith, J.N. Israelachvili, J.H. Waite, Mussel-inspired adhesives and coatings, Annu. Rev. Mater. Res. 41 (2011) 99–132.
[43] S. Hajebi, S. Mohammadi Nasr, N. Rabiee, M. Bagherzadeh, S. Ahmadi, M. Rabiee, M. Tahriri, L. Tayebi, M.R. Hamblin, Bioresorbable composite polymeric materials for tissue engineering applications, Int. J. Polym. Mater. Polym. Biomater. (2020) 1–15.
[44] J.M. Andrews, BSAC standardized disc susceptibility testing method, J. Antimicrob. Chemother. 48 (Suppl. 1) (2001) 43–57.
[45] M. Balouiri, M. Sadiki, S.K. Ibnsouda, Methods for in vitro evaluating antimicrobial activity: a review, J. Pharm. Anal. 6 (2) (2016) 71–79.
[46] J. Théolier, R. Hammami, P. Labelle, I. Fliss, J. Jean, Isolation and identification of antimicrobial peptides derived by peptic cleavage of whey protein isolate, J. Funct. Foods 5 (2013) 706–714.
[47] T. Rozario, D.W. DeSimone, The extracellular matrix in development and morphogenesis: a dynamic view, Dev. Biol. 341 (1) (2010) 126–140.
[48] H.C. Blair, Q.C. Larrouture, Y. Li, H. Lin, D. Beer-Stoltz, L. Liu, R.S. Tuan, L. J. Robinson, P.H. Schlesinger, D.J. Nelson, Osteoblast differentiation and bone matrix formation in vivo and in vitro, Tissue Eng. B Rev. 23 (3) (2017) 268–280.
[49] A. Jukkola, L. Risteli, J. Melkko, J. Risteli, Procollagen synthesis and extracellular matrix deposition in MG-63 osteosarcoma cells, J. Bone Miner. Res. 8 (6) (1993) 651–657.
[50] D. Benayahu, I. Shur, R. Marom, I. Meller, J. Issakov, Cellular and molecular properties associated with osteosarcoma cells, J. Cell. Biochem. 84 (1) (2001) 108–114.
[51] S. Murad, D. Grove, K.A. Lindberg, G. Reynolds, A. Sivarajah, S.R. Pinnell, Regulation of collagen synthesis by ascorbic acid, Proc. Natl. Acad. Sci. 78 (5) (1981) 2879–2882.
[52] K. Parkatzidis, M. Chatzinikolaidou, M. Kaliva, A. Bakopoulou, M. Farsari, M. Vamvakaki, Multiphoton 3D printing of biopolymer-based hydrogels, ACS Biomater. Sci. Eng. 5 (11) (2019) 6161–6170.
[53] F. Erpel, R. Mateos, J. Perez-Jimenez, J.R. Perez-Correa, Phlorotannins: from isolation and structural characterization, to the evaluation of their antidiabetic and anticancer potential, Food Res. Int. 137 (2020).
[54] K. Gkioni, S.C.G. Leeuwenburgh, T.E.L. Douglas, A.G. Mikos, J.A. Jansen, Mineralization of hydrogels for bone regeneration, *Tissue Eng. B Rev.* 16 (6) (2010) 577–585.
[55] T.E. Douglas, P.B. Messersmith, S. Chasan, A.G. Mikos, E.L. de Mulder, G. Dickson, D. Schaubroeck, L. Balcaen, F. Vanhaecke, P. Dubruel, J.A. Jansen, S. C. Leeuwenburgh, Enzymatic mineralization of hydrogels for bone tissue engineering by incorporation of alkaline phosphatase, Macromol. Biosci. 12 (8) (2012) 1077–1089.
[56] N.D. Evans, C. Minelli, E. Gentleman, V. LaPointe, S.N. Patankar, M. Kallivretaki, X. Chen, C.J. Roberts, M.M. Stevens, Substrate stiffness affects early differentiation events in embryonic stem cells, Eur. Cells Mater. 18 (2009) 1–13 (discussion 13-4).
[57] B.D. Boyan, S. Lossdörfer, L. Wang, G. Zhao, C.H. Lohmann, D.L. Cochran, Z. Schwartz, Osteoblasts generate an osteogenic microenvironment when grown on surfaces with rough microtopographies, Eur. Cells Mater. 6 (2003) 22–27.